physica status solidi

pss

www.pss-journals.com

reprint

WILEY-VCH

Wiley Online Library
Early View publication on www.wileyonlinelibrary.com
(issue and page numbers not yet assigned;
citable using Digital Object Identifier – DOI)

Phys. Status Solidi A, 1–7 (2015) / DOI 10.1002/pssa.201431829

physica status solidi a
www.pss-a.com
applications and materials science

Fully flexible and transparent piezoelectric touch sensors based on ZnO nanowires and $BaTiO_3$-added SiO_2 capping layers

MoolKyul Kang[1,2], Jae Hyun Park[1], Kyoung Il Lee[1], Jin Woo Cho[1], Joonho Bae[3], Byeong Kwon Ju*[,2], and Churl Seung Lee*[,1]

[1] Energy and Nanomaterial Research Center, Korea Electronics Technology Institute, Seongnam 463-816, Korea
[2] Display and Nanosystem Laboratory, College of Engineering, Korea University, Seoul 136-713, Korea
[3] Department of Nano-Physics, Gachon University, Seongnam 461-701, Korea

Received 13 November 2014, revised 18 February 2015, accepted 20 March 2015
Published online 23 April 2015

Keywords $BaTiO_3$, capping layers, flexible devices, nanowires, optical transparency, piezoelectric properties, touch sensors, ZnO

* Corresponding authors: e-mail assong@keti.re.kr; bkju@korea.ac.kr, Phone/Fax: 0041 263009624

We report on fully flexible and transparent piezoelectric touch sensors based on ZnO nanowires (NWs). Their piezoelectric properties are further enhanced by incorporating $BaTiO_3$ into the capping layer on nanowires. Flexibility is improved by a highly transparent carbon nanotubes–silver nanowires electrode. A $BaTiO_3$-based capping layer on ZnO nanowires demonstrates a large increase of the output voltage (~3.3 V) from the touch sensor compared to the voltage (~50 mV). Mechanical bending tests reveal that the $BaTiO_3$-added capping layer did not show significant degradation in change of resistance. Our results suggest that the piezoelectric touch sensors are promising for next-generation flexible touch sensors, wearable, and rollable touch panels.

1 Introduction Recently, studies on flexible devices have become intensive since their shapes are variable with the advantages of diverse device areas, lightweight, and robustness [1]. The flexible transparent electrodes have been one of the most important materials used in flexible devices such as flexible touch sensors [2], nanogenerators [3], and displays [4]. In general, most electronic devices have used indium tin oxide (ITO) as a transparent flexible electrode by sputtering because of its high conductivity and high transmittance in the visual region. However, due to a lack of flexibility of the ITO films, their alternatives are being investigated [5]. Currently, conductive films using carbon nanotubes and Ag nanowires are considered as prospective replacements of ITOs.

It is noteworthy that the reports on ZnO nanowires (NWs) as conductive electrodes are growing in the literature. The ZnO NWs show extremely high flexibility and have many degrees of mechanical deformation without cracking or fracture [6]. The ZnO NWs have several benefits for use in electronic device because of high flexibility, low cost, and being ultrathin and easy to fabricate for nanogenerators [7] and sensing devices [8]. In addition, the ZnO NWs can be grown via the hydrothermal method at low temperatures (<100 °C), resulting in the versatile availability of various substrates. However, conventional piezoelectric devices based on ZnO NWs are reported to demonstrate limited piezoelectric properties due to the low piezoelectric d constant of ZnO NWs ($d \simeq 12$ pC/N) [9, 10].

In this paper, we report a fully flexible and transparent piezoelectric touch sensor based on ZnO NWs. Its piezoelectric properties are improved by fabricating the touch sensor using perovskite piezoelectric $BaTiO_3$. The perovskite ceramic materials ($PbZr_xTi_{1-x}O_3$, $d \simeq 400$ pC/N and $BaTiO_3$, $d \simeq 270$ pC/N) have a high level of inherent piezoelectric properties [11, 12]. Since their brittleness hinders their use as electrodes for the flexible devices, we fabricated a ZnO NW capping layer after having dispersed $BaTiO_3$ in a flexible SiO_2-added capping solution in order to maintain the flexibility of sensing components. Using these capping layers, we significantly enhanced the flexibility and

permeability of the touch sensors, and demonstrated touch-sensitive piezoelectric sensors with high output voltage.

2 Experimental

2.1 Fabrication of the flexible touch sensors To fabricate the flexible touch sensors, poly(ethylene terephthalate) (PET) flexible substrates with thickness of 188 μm were cleaned in acetone, ethanol, and deionized water for 10 min and dried with nitrogen gas (Fig. 1a). We coated the CNT-Ag NWs solution (18 mL) as a bottom electrode on the PET substrates using the spray-coating method (Fig. 1b). After the coating process, the sensing buttons were patterned on the substrates using photolithography. Negative photoresist SU-8 2002 (Microchems) was spun at 3000 rpm for 2 min on CNT-Ag NWs coated substrates, subsequently baked at 90 °C for 20 s (Fig. 1c).

The photoresist-coated substrates were exposed to UV light for 30 s using a contact mask aligner, and post-exposure bake was performed at 90 °C for 5 min (Fig. 1d) after the exposure. After the photoresist development process, the substrates were hard-baked at 150 °C, for 5 min (Fig. 1e). The pattern serves as a mask for ZnO NWs selectively grown on the bottom electrode. An aluminum-doped ZnO (AZO) seed layer (~50 nm) is sputtered on the patterned PETs using RF magnetron sputtering at room temperature (Fig. 1f). To fabricate the sensing buttons, ZnO NWs were grown on a patterned PET substrate via the hydrothermal method (see Supporting Information, online at: www.pss-a.com) as shown in Fig. 1g. In order to retain the flexibility of the sensing button, we fabricated a capping layer on top of the ZnO NWs as follows. First, barium titanate(IV), nanopowder ($BaTiO_3$, <100 nm particle size, Sigma Aldrich) was dispersed at the concentration of 10 wt.% in silsesquioxane (SSQ)-based SiO_2 capping solution (Fig. 1h). The flexibility of the SiO_2 capping coating solution was controlled by increasing the polysilizane concentration in the solution. The capping layer was then coated on the top layer of the film formed by ZnO NWs by using a nanospray coating system. In order to improve the flexibility of the entire device, we coated the solution containing CNT-Ag NWs (18 mL) by using a spray-coating system on the capping layer to form a top electrode (Fig. 1i).

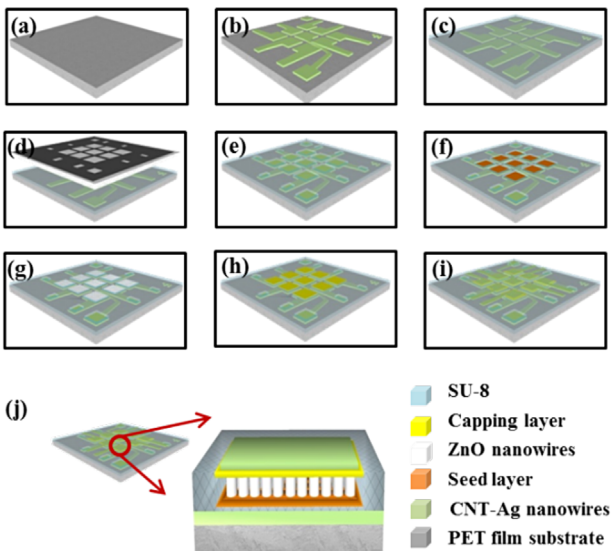

Figure 1 Schematic illustration of the fabrication process for the piezoelectric touch sensor. (a) Washing of PET film substrate. (b) Spray coating of CNT-Ag NWs (bottom electrode) a PET substrate. (c) Spin coating of negative photoresist (SU-8 2002) CNT-Ag NWs on PET substrate. (d) Patterned negative photoresist formation. (e) Fabricating a sensing point by photolithography. (f) Deposition of an aluminum-doped ZnO seed layer. (g) Growth of ZnO NWs on the sensing point. (h) Spray coating of a capping layer on the ZnO NWs and (i) CNT-Ag NWs (top electrode). (j) Cross-sectional image of the touch-point structure.

2.2 Surface characterization Surface morphology examination was performed by field emission scanning electron microscopy (JSM-7000F) typically operated at 10 kV.

2.3 Mechanical bending tests Mechanical bending tests were carried out with a mechanical bending tester (KETI-made).

3 Results and discussion Figure 2a shows a cross-sectional SEM image of the ZnO NWs grown on a PET substrate. The ZnO NWs have length of 900 nm and diameter of 120 nm. It is seen that the nanowires are vertically grown with a high density, seeming like a polycrystalline thick film on the PET substrate. The elemental analysis of touch buttons was also performed by using energy-dispersive spectroscopy (EDS) (Fig. 2b). The EDS analysis result confirms that the NWs are composed of Zn and O (Fig. 2b). Figure 2c shows a cross-sectional SEM image of the touch buttons. The $BaTiO_3$-added capping layer is shown to uniformly cover the ZnO NWs. Figure 2c illustrates that CNT-Ag NWs have been formed a top electrode on top of the capping layer. Figure 2e shows a result from EDS elemental mapping on the flexible capping layer. The yellow dots representing Si contents show the region of the capping layer. The densely-populated dots (yellow color) in the upper region confirmed the formation of the capping layer. Interestingly, the same yellow dots are observed in the middle region of the image, suggesting that SiO_2 capping solution has permeated to the ZnO NW region. The yellow dots at the bottom are due to the SiO_2 glass used as substrates for SEM measurement (Supporting Information). Figure 2f shows the EDS elemental mapping of Ba content, indicating that the $BaTiO_3$ nanoparticles are uniformly distributed in the flexible capping layer (green dots).

To test the mechanical durability of our touch sensors, we performed a monitoring of resistance measurements of the capping layers and touch sensor while they underwent repeated mechanical bending in a KETI-made bending test equipment. The bending test reveals the high mechanical durability of the capping layer and touch sensor. The mechanical bending tests take place by connecting two ends of each sample to a corresponding clamp, followed by

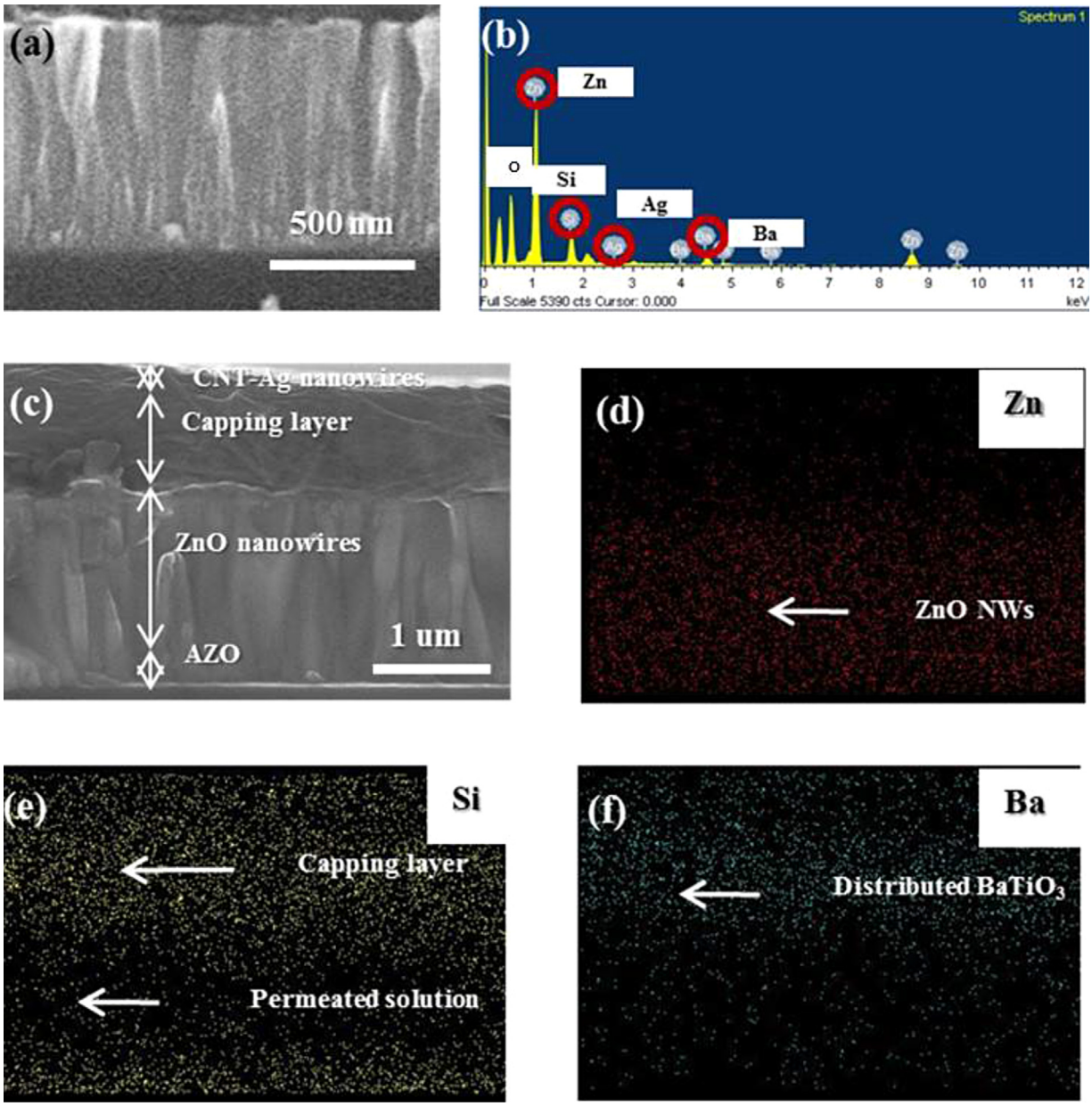

Figure 2 (a) Cross-sectional SEM image of ZnO NWs. (b) EDS spectra of touch-point structure. (c) Cross-sectional SEM image of touch-point structure. EDS images of elemental mapping showing, (d) ZnO NWs, (e) Si content in the capping layer, and (f) $BaTiO_3$ content in the capping layer.

moving one of the clamps to generate the bending effect (see inset in Fig. 3). The bending action is repeated 1000 times at the bending angle of 30°. The resistance of the samples is monitored by a resistance meter during the entire bending process.

In order to investigate the influence of $BaTiO_3$ on the flexibility of the capping layers, the bending experiments were performed on three kinds of capping layers formed on the flexible PET substrates. The capping layers are (i) bare capping layer (conventional SiO_2 capping solution), (ii) flexible capping layers whose flexibility is controlled by increasing the polysilizane concentration compared to the bare capping solution, and (iii) capping layers $BaTiO_3$ added in the flexible capping solution. All three layers are deposited on flexible PET substrates at a thickness of 500 nm.

Figure 3 presents the results of the bending experiments performed on the bare capping layers. The change of resistance of the capping layer is defined as

$$\Delta R(\%) = \left\{\frac{(R - R_0)}{R_0}\right\} \times 100, \quad (1)$$

where R_0 is the initial resistance before the bending test and R is the resistance measured during the bending test.

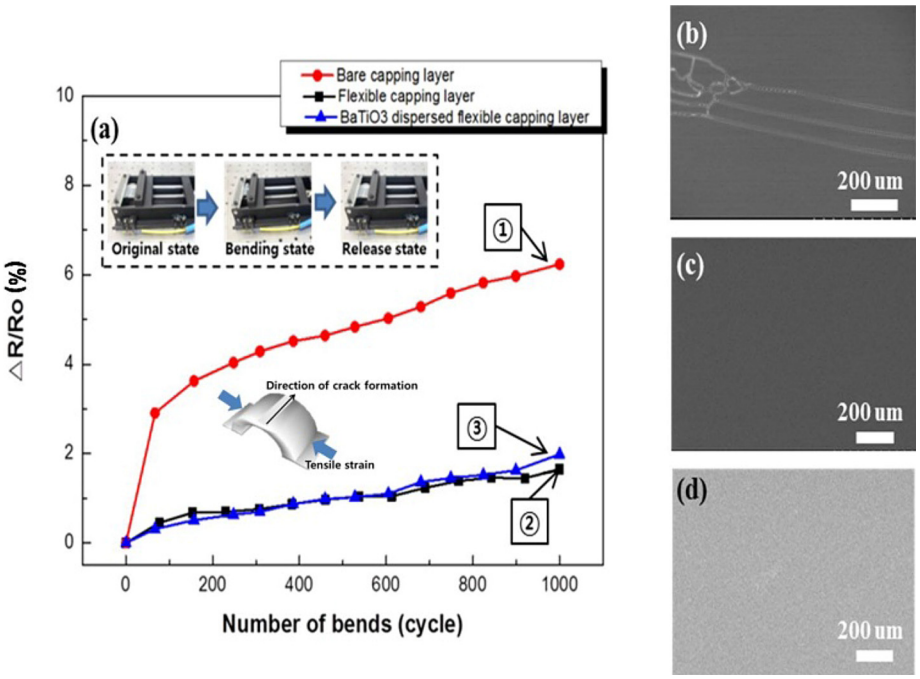

Figure 3 (a) Change in resistance of the capping layer under mechanical bending. Top-view SEM images of (b) the bare capping layer after a 1000-cycle bending test, showing the delamination from PET substrate and (c) the flexible capping layer after a 1000-cycle bending test. (d) Top-view SEM image of the $BaTiO_3$-added capping layer.

Figure 3a shows the change in resistance of three capping layers. When bent and flexed over 1000 cycles, the bending angle of the substrates is 30°, the flexible capping layer (1.7%) and $BaTiO_3$-added flexible capping layer (1.9%) did not show significant degradation in resistance compared to the bare capping layer (6.7%). At the bending angle of 30°, the strain is calculated to be 0.375% (Supporting Information). At 80 cycles, the resistance of the bare capping layer began to increase. By contrast, the change in resistance of the flexible capping layer did not demonstrate a significant change (~0.04%). The SEM image reveals that a crack has been formed on the surface in the bare capping layer (Fig. 3b) while the flexible capping layer did not show any crack (Fig. 3c and d). After 80 cycles, cracks began to form on the surface of the bare capping layer. Then, the cracks propagated on the capping layer, resulting in the significant damage of the whole substrate. Hence, the cycle of 80 can be considered as a threshold cycle in which the failure of the capping layer begins to occur. This result suggests that the resistance tends to decrease with increasing flexibility of the capping layer. After 1000 cycles, FE-SEM reveals that only the bare capping layer showed significant crack formation, indicating that the adhesion property and durability of the ZnO NWs were enhanced by coating the flexible capping layer on the ZnO NWs (see Supporting Information, Fig. S1).

Using the ZnO NWs and $BaTiO_3$-added capping layers, we fabricated a single touch-point cell ($1 \times 1\,cm^2$) using the same process as those for the touch sensors with nine cells (Fig. 4a). During the bending test from 100 to 2000 cycles, we measured the voltage generated from the touch sensor. The durability tests and voltage measurement revealed that the output voltage did not change up to 2000 cycles of bending. The touch sensor

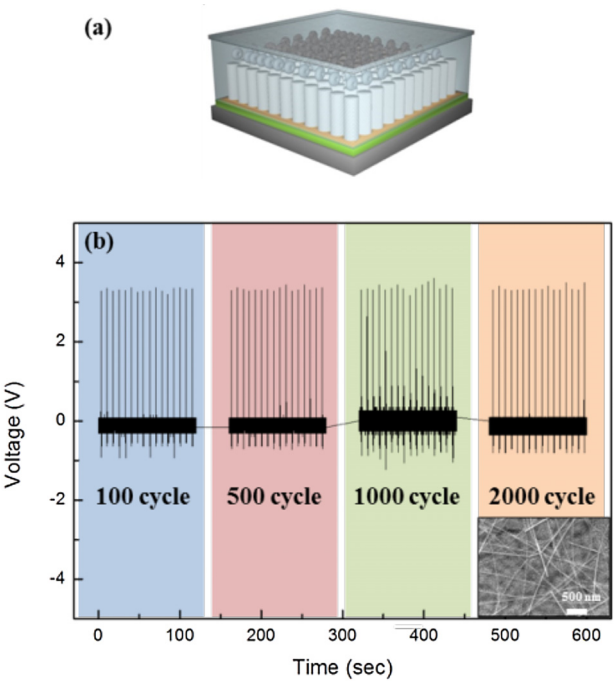

Figure 4 (a) Schematic illustration of a single touch-point cell, (b) durability test of a touch sensor. The inset: SEM image of the sensor.

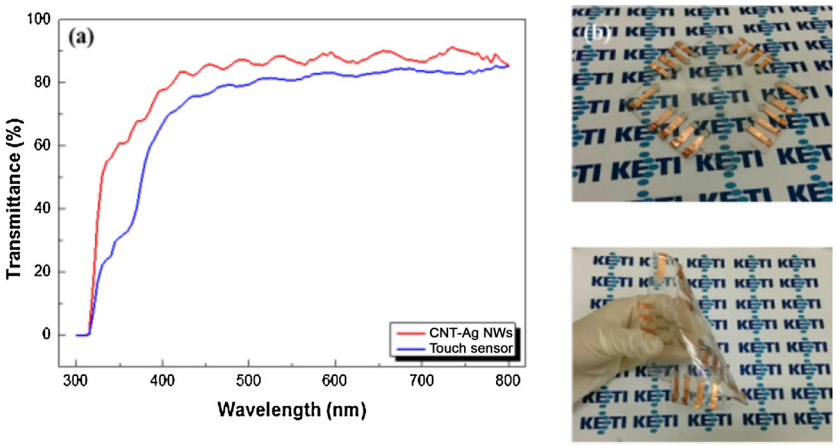

Figure 5 (a) Optical transmittance spectra from CNT-Ag NWs and our touch sensor. (b) Photo of a piezoelectric touch sensor showing the KETI logo.

generates the output voltage of ~3.3 V during 2000 cycles (Fig. 4b). After 2000 cycles, we examined the surface morphology of the touch sensor via SEM (the inset in Fig. 4b). In the SEM image of the inset in Fig. 4b, no crack is observed in the touch sensor, indicating excellent mechanical stability of the touch sensor.

To characterize the optical performance, transmittance measurements were performed on the capping layer and

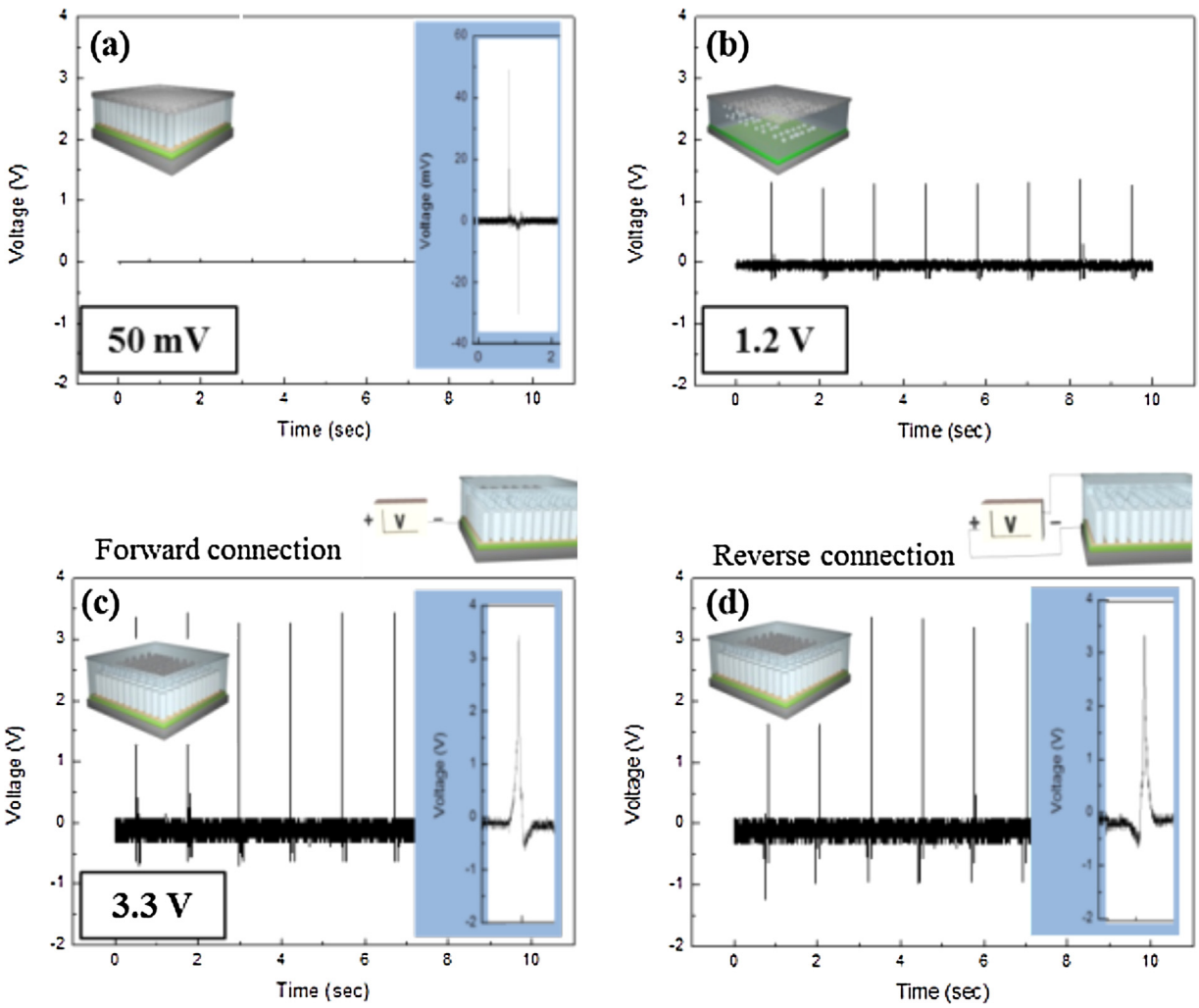

Figure 6 Operating characteristic of (a) ZnO NW added touch sensor. (b) $BaTiO_3$-added touch sensor and (c) $BaTiO_3$-added ZnO NW-based touch sensor. (d) Output voltages generated in the reversed connection mode.

whole touch sensor. As shown in Fig. 5, ITO, the conventional transparent electrode showed 73% at 550 nm. The CNT-Ag NWs electrode exhibits a higher transmittance of ~83%. It is seen that the transmittance of the whole device was almost unchanged (81% at 550 nm). Figure 5b shows a photo of a touch sensor with KETI logo, indicating its high optical transparency and mechanical flexibility.

Figure 6 shows the output voltage of the touch sensor with three different configurations. When a linear motor exerted a force of 17 N, the output voltages from the ZnO NW-based sensor and $BaTiO_3$-based sensor generated the output voltages of ~50 mV and ~1.2 V, respectively (Fig. 6a). $BaTiO_3$-based sensor generated output voltage increasing from 0.024 to 1.2 V after the poling process (Supporting Information, Fig. S2). The maximum output voltage from the touch sensor with $BaTiO_3$-added ZnO NWs hybrid structure is up to 3.3 V (Fig. 6c). The piezoelectric output voltage is calculated as

$$V = \frac{F \cdot d_{33} \cdot T}{W \cdot L}, \tag{2}$$

where V is the output voltage, F is the pressure force, d_{33} the piezoelectric coefficient, T the thickness of the piezoelectric layer, W the width, and L the length of the piezoelectric layer. Since d_{33} values of $BaTiO_3$ and ZnO NWs are 270 and 19 pC/N, respectively, $BaTiO_3$ could exhibit output voltages 20 times larger than those from ZnO NWs according to the equation above. The output voltage of the sensor with $BaTiO_3$ was 1.2 V. This voltage value is about 24 times that of ZnO NWs-based sensor (50 mV), which is in accordance with Eq. (2).

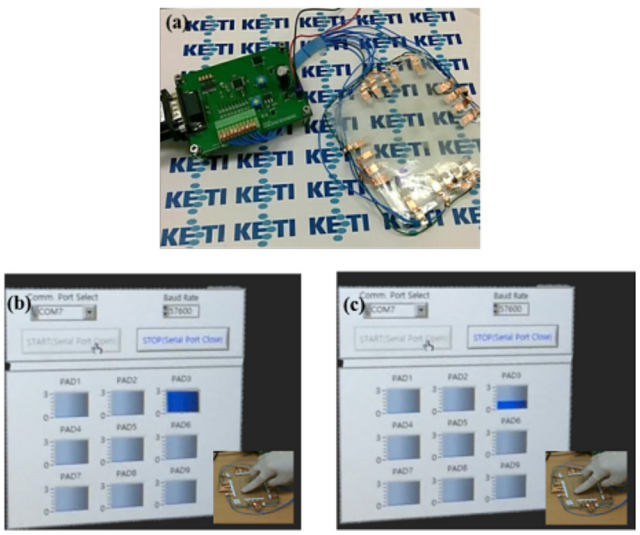

Figure 7 (a) Photograph of a piezoelectric touch sensor connected with an amplifier circuit for converting mechanical energy into an output voltage. (b) Display of a fully blue square in screen when the sensor is hard pressed. (c) Display of a partly filled blue square when the sensor is lightly pressed.

In addition, the switching polarity test conducted on the touch sensors demonstrated that the output voltages are not artifacts and generated only from the sensors (Supporting Information, Fig. S3) [13–18].

We fabricated a touch sensor by arraying nine cells on PETs. An impedance converter circuit was connected to the piezoelectric touch sensor (Fig. 7a). The display characteristics on the monitor were investigated by pressing one of the touch points (Fig. 7b and c). We also examined the display behavior of the touch point at different pressing forces. When the touch point is pressed hard, the resultant display is filled fully with blue color. On the other hand, the display is half-filled with blue color on light pressing. Hard and light pressing motions induce the deformation of the touch sensor to different extents, resulting in different touch-sensitive displays.

4 Conclusions In conclusion, we have successfully demonstrated a fully flexible and transparent piezoelectric touch sensor based on ZnO NWs. By replacing ITO electrodes with transparent flexible CNT-Ag NWs electrodes, we enhanced the flexibility of the entire device structure. We demonstrated that the output voltage of the sensor with $BaTiO_3$-added ZnO NWs was significantly increased. The excellent flexibility of the capping layer with $BaTiO_3$ and a CNT-Ag NWs electrode enabled us to fabricate a piezoelectric touch sensor with high electrical and mechanical stability. Our piezoelectric touch sensors could be promising for flexible devices such as flexible touch sensors, or wearable, and rollable touch panels.

Supporting Information

Additional supporting information may be found in the online version of this article at the publisher's website.

Acknowledgements This work was supported by the Graphene Materials/Components Development Project (10044366) funded by the Ministry of Trade, industry and Energy (MOTIEI, Korea). This research was supported by Basic Science Research Program through the National Research Foundation of Korea (NRF) funded by the Ministry of Science, ICT and Future Planning (2013R1A1A1008436) (JB).

References

[1] K. A. Sierros, D. A. Banerjee, N. J. Morris, D. R. Cairns, I. Kortidis, and G. Kiriakidis, Thin Solid Films **518**, 325 (2010).
[2] C. Rendl, P. Greindl, M. Haller, M. Zirkl, B. Stadlober, and P. Hartmann, in: Proc. 25th Annual ACM Symposium on User Interface Software and Technology, 2012, p. 509.
[3] D. H. Choi, M. Y. Choi, H. J. Shin, S. M. Yoon, J. S. Seo, J. Y. Choi, S. Y. Lee, J. M. Kim, and S. W. Kim, J. Phys. Chem. C **144**, 1379 (2010).
[4] P. C. Wang and A. G. MacDiarmid, Displays **28**, 101 (2007).
[5] K. A. Sierros, D. S. Hecht, D. A. Banerhee, N. J. Morris, L. Hu, G. C. Irvin, R. S. Lee, and D. R. Cairns, Thin Solid Films **518**, 2677 (2010).
[6] Z. L. Wang, Nano Today **5**, 540 (2010).

[7] G. Zhu, A. C. Wang, Y. Lin, Y. Zhou, and Z. L. Wang, Nano Lett. **12**, 3086 (2012).
[8] D. Choi, K. Y. Lee, K. H. Lee, E. S. Kim, T. S. Kim, S. Y. Lee, S.-W. Kim, J.-Y. Choi, and J. M. Kim, Nanotechnology **21**, 405503 (2010).
[9] Y. H. Wang, X. Li, C. Zhao, and X. Liu, in: Proc. 27th IEEE International Conference on Micro-Electro Mechanical Systems, 2014, p. 782.
[10] J. H. He, C. L. Hsin, J. Liu, L. J. Chen, and Z. L. Wang, Adv. Mater. **19**, 781 (2007).
[11] F. Xia and X. Yao, J. Mater. Sci. **34**, 3341 (1999).
[12] H. Takahashi, Y. Numamoto, J. Tani, K. Matsuta, J. Qiu, and S. Tsurekawa, Jpn. J. Appl. Phys. **45**, L30 (2006).
[13] R. Yang, Y. Qin, L. Dai, and Z. L. Wang, Appl. Phys. Lett. **94**, 022905 (2009).
[14] J. W. Cho, C. S. Lee, K. I. Lee, S. M. Kim, S. H. Kim, and Y. K. Kim, Appl. Phys. Lett. **101**, 083905 (2012).
[15] D. H. Choi, M. Y. Choi, W. M. Choi, H. J. Shin, H. K. Park, J. S. Seo, J. B. Park, S. M. Yoon, S. J. Chae, Y. H. Lee, S. W. Kim, J. Y. Choi, S. Y. Lee, and J. M. Kim, Adv. Mater. **22**, 2187 (2010).
[16] K. I. Park, M. B. Lee, Y. Liu, S. Moon, G. T. Hwang, G. Zhu, J. E. Kim, S. O. Kim, D. K. Kim, and K. J. Lee, Adv. Mater. **24**, 2999 (2012).
[17] E. S. Choi, J. O. Kim, S. W. Chun, A. S. Kim, K. H. Lee, M. H. Jeong, Ch. H. Lim, T. Isoshima, M. Kara, and S. B. Lee, J. Nanosci. Nanotechnol. **11**, 5845 (2011).
[18] A. F. Yu, H. Y. Li, H. Y. Tang, T. J. Liu, P. Jiang, and Z. L. Wang, Phys. Status Solidi RRL **5**, 162 (2011).